forests

Article

Experimental Analysis on the Behaviors of a Laboratory Surface Fire Spreading across a Firebreak with Different Winds

Hanwen Guo, Zhengyuan Yang, Ziqun Ye, Dong Xiang, Yunji Gao * and Yuchun Zhang *

Department of Fire Protection Engineering, Southwest Jiaotong University, Chengdu 610031, China; hanwenguo@my.swjtu.edu.cn (H.G.); yangzy999@my.swjtu.edu.cn (Z.Y.); xd99@my.swjtu.edu.cn (D.X.)
* Correspondence: gyj119@swjtu.edu.cn (Y.G.); zycfire@home.swjtu.edu.cn (Y.Z.)

Abstract: In this work, a series of laboratory surface fire experiments were performed over a pine needle fuel bed to investigate the effectiveness of a firebreak and the behaviors of a surface fire across a firebreak. Seven wind velocities of 0~3.0 m/s and six firebreak widths of 10~35 cm are varied. The behaviors of a surface fire across the firebreak, the heat flux received by fuel surface and fuel temperature before and after the firebreak are analyzed and compared simultaneously. The main conclusions are as follows: the behaviors of a surface fire spreading across a firebreak under different wind velocities are classified into three categories—no ignition, ignition by flame contact and ignition by spot fires. When the wind velocity is not more than 1.0 m/s, the surface fire cannot successfully cross the firebreak; as wind velocity changes from 1.5 m/s to 2.5 m/s, the fuel after the firebreak can be ignited by flame contact for relatively narrow firebreak conditions; when the wind velocity increases to 3.0 m/s, the burning fuel can be blown away along the fuel bed, and the fuel behind the firebreak will be ignited by spot fire. A linear relationship between the threshold of firebreak width and the fireline intensity is obtained, and the linear fitting coefficient in this paper is larger than the results reported by Wilson (0.36). For no ignition conditions, the fuel temperature and the heat flux received by the fuel after firebreak are significantly lower than those before the firebreak, whereas their variations over time are similar to those before the firebreak for ignition conditions. Moreover, for no ignition conditions, the maximum fuel temperature and the heat flux after the firebreak increase with wind velocity, but decrease with firebreak width. Additionally, when the fuel temperature (253 °C) and the heat flux received by the fuel considering the radiation and convection (43 kW/m^2) after firebreak exceed a threshold value, the surface fire can successfully cross the firebreak.

Keywords: firebreak; surface fire spread; wind velocity; heat flux

check for updates

Citation: Guo, H.; Yang, Z.; Ye, Z.; Xiang, D.; Gao, Y.; Zhang, Y. Experimental Analysis on the Behaviors of a Laboratory Surface Fire Spreading across a Firebreak with Different Winds. *Forests* **2023**, *14*, 2455. https://doi.org/10.3390/f14122455

Academic Editor: Cate Macinnis-Ng

Received: 23 October 2023
Revised: 21 November 2023
Accepted: 6 December 2023
Published: 17 December 2023

1. Introduction

Forests can provide a number of ecological services, including enhanced infiltration and water retention, which will contribute to improving the water quality and reducing the flood hazard [1]. In addition, forest fires pose a significant threat to human life [2]. Molina-Terren et al. [3] pointed out that firefighting professionals and civilians lose their lives in forest fires every year by assembling and examining a database of civilian and firefighter forest-fire fatalities in four regions in Mediterranean Europe. In recent decades, global warming and the increase of extreme weather have led to the frequent occurrence of forest fires, consequently causing ecological losses [4]. As is well known, surface fires are the most frequent type of forest fires and one of the main causes of canopy fires, which have gradually received considerable attention. Rothermel et al. [5] experimentally studied the slope effects on surface fire spread and proposed an empirical formula to estimate the fire spread rate considering the terrain slope effects. Catchpole et al. [5] conducted a series of experiments in a wind tunnel to investigate the wind effects on surface fire spread, and established a predictive model for fire spread rate. Viegas [6] pointed out that slope and wind were dominant factors affecting the spread of forest fires, and carried out theoretical and experimental research on the vectoring of the wind and slope effects on a flame front. Subsequently, the effects of weather [7–10] and topography [7,8,11–21], the key factors in fire triangles (fuel/weather/topography) at the wildfire level, on surface fire spread behavior and heat transfer mechanism have been extensively studied. However, compared with these in-depth studies on ignition and fire behaviors, very few investigations are reported on controlling surface fire spread in wildfires.

With respect to the fire triangle at the wildfire level, no action can be taken against the weather and topography, and the only means of reducing fire intensity and fire risk is to reduce the fuel load [22]. This method can contribute to achieving various objectives of reducing the fire intensity and decreasing the impact of a wildfire on a forest or on the wildland-urban interface [22]. A firebreak, where the fuel load is reduced by removing all or part of the fuel, is a typical strategy to prevent the fire from escaping the burning area and igniting the unburned fuel. A firebreak has been applied in the management of wildfires to reduce the fire spread rate, fire size and fire intensity [23]. Emmons [24] firstly put forward a physical model to estimate the threshold of firebreak width to build a safety zone. Wilson [25] carried out a series of experiments to investigate the effectiveness of firebreaks under different firebreak width conditions, and developed a prediction model for the threshold of firebreak width. However, he focused on the effects of fireline intensity and rate of spread on the effectiveness of the firebreak, but paid little attention to the flame angle, fuel surface temperature and heat transfer control mechanisms during surface fire spread across the firebreak. Recently, Morvan et al. [26] investigated the behaviors of a surface fire propagating a firebreak by two-dimensional numerical simulations, and found that above a threshold firebreak width, even if the fire was able to ignite the driest fuel on the opposite side of the firebreak, the energy released was not sufficient to sustain the surface fire spread. Moreover, the spread behaviors of a crown fire and the efficiency of a fuel break were numerically tested [27]. Frangieh et al. [22] studied the effectiveness of a firebreak against wind-driven and plume-dominated fires using a detailed physical-fire-model, and the spread results were classified into three main categories of propagation, overshooting, marginal and no propagation. However, most of the existing studies are mainly based on numerical simulations, and very little work has been reported using experimental methods. Additionally, most previous work did not pay attention to the changes of heat flux received by fuel and fuel temperature before and after the firebreak, especially in the case of wind or terrain slope, where flames would be elongated and tilted, the heat flux from flames and behaviors of a surface fire across a firebreak would change.

Ambient wind, one of the key factors affecting the spread of surface fires, has been studied quite extensively in previous work [7–10]. As is well known, the wind would enhance heat transfer and increase the fire spread rate in wildfires. Therefore, the purpose of this paper is to study the effectiveness of the firebreak, and compare the behaviors of a surface fire before and after the firebreak. A series of laboratory scale fire experiments were carried out over a pine needle fuel bed. Seven wind velocities and six firebreak widths were varied. The essential parameters were obtained and analyzed, including the behavior of a surface fire across the firebreak, the heat flux received by the fuel surface and the fuel surface temperature before and after the firebreak. The results in this paper are helpful for better understanding the firebreak effectiveness and the ignition mechanism of the fuel on the opposite side of the firebreak.

2. Experimental Setup

Figure 1 schematically presents an experimental setup for surface fire experiments, which is an open-topped tunnel measuring 6.0 m long, 3.0 m wide and 2.0 m high. A fireproof glass was installed on one side of the setup for recording the surface fire spread, but a steel plate was selected to be installed on the other side. The fuel bed was 3.0 m long and 1.5 m wide without retaining walls along the lengthwise perimeter, and was divided into the three following sections: the firebreak, fuel before the firebreak and fuel after the firebreak. The fuel of surface fire was placed on a support panel consisting of three 0.08 m thick fireproof boards (density 400 kg/m^2 and thermal conductivity 0.1 W/(m·°C)) to minimize heat loss during the propagation of surface fire. The firebreak was positioned 2.0 m away from the start of the fuel bed, and the width of firebreak was manually adjusted towards the rear of the fuel bed. The specific wind velocity was acquired by a variable frequency fan, which was positioned on the left side of the fuel bed. Moreover, the influence of airflow turbulence from the fan was reduced by the combination of honeycomb and screens, which was also chosen by Tachajapong [9,28]. All experiments were conducted in a large test hall with ambient temperature of 25.2 ± 2 °C and relative humidity of 62 ± 5%.

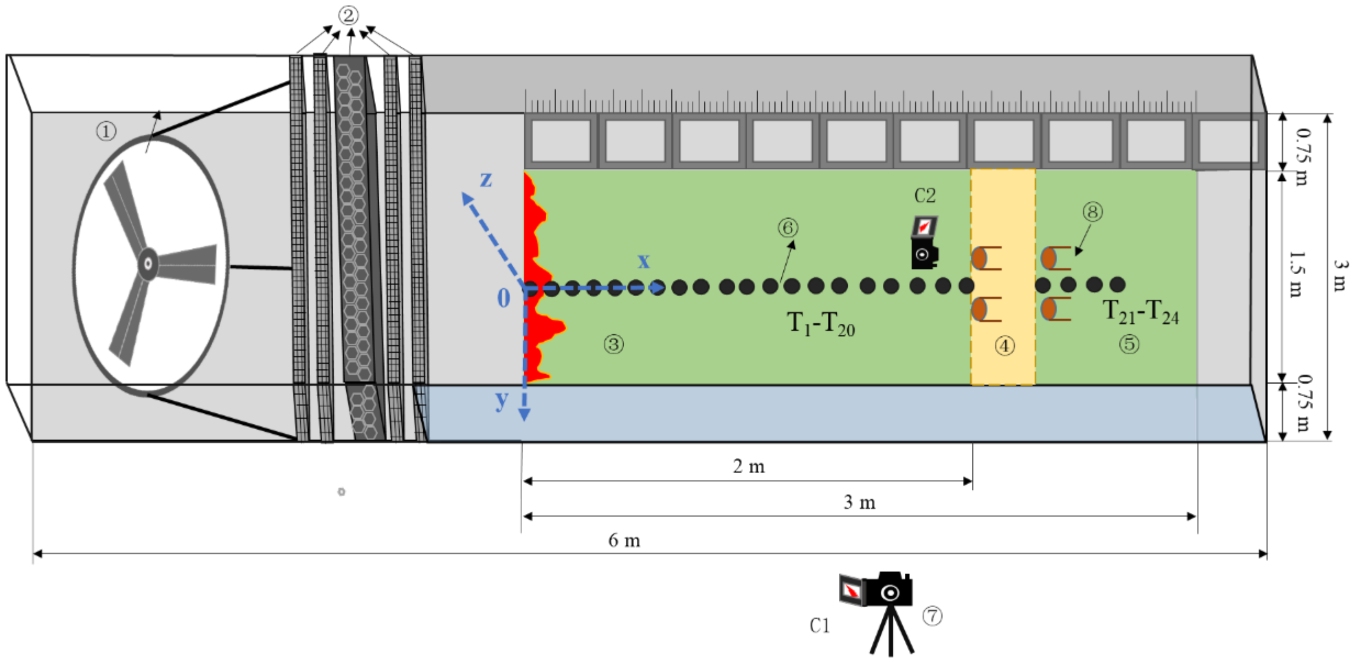

Figure 1. Schematic diagram of the experimental setup. ① Inverter fans; ② combination of honeycomb and screens; ③ fuel before firebreak; ④ firebreak; ⑤ fuel after firebreak; ⑥ thermocouple; ⑦ camera; ⑧ heat flux sensors.

In order to get sufficient information for the measurements, a three-dimensional coordinate system was created on the fuel bed as shown in the following figure. In this coordinate system, x = 0 is the beginning of the fuel bed towards the spread of the fire, y = 0 is the centerline of the fuel bed, z = 0 is the surface of the substrate. The temperature over the fuel was obtained by K-type thermocouples, which were installed 3.0 cm above the fuel. For the fuel section before firebreak, 20 thermocouples were arranged horizontally at 10 cm intervals from the beginning to the front of the firebreak along the centerline axis, which are labelled as T_1~T_{20}. The other 4 thermocouples, labelled as T_{21}~$T_{24,}$ were placed horizontally at 10 cm intervals in the fuel section after firebreak. The temperature measurement range and diameter of thermocouples were 0~1100 °C and 1.0 mm, respectively. Two 4K cameras (Sony FDR-AX60 from Chengdu, China) with a resolution of 1920 × 1080 and a frame rate of 25 fps were set up to observe and record the surface fire spread process characteristics from two directions. The sideview camera was arranged at x = 150 cm, y = 300 cm, z = 0 cm to record the flame geometry of the surface fire through the fire glass, while the other camera was positioned at x = 200 cm, y = 0 cm, z = 200 cm to record the surface fire spread and the effectiveness of the firebreaks from an overhead viewpoint. The heat fluxes of total and radiation heat flux were obtained at different positions including before and after the firebreak by a total heat flux sensor (range 0–100 kW·m^{-2}, response time 300 m·s, view 150°) and a radiation heat flux sensor (range 0–50 kW·m^{-2}, response time 300 m·s, view 150°). The faces of the sensors were positioned flush with the top surface of the fuel and facing upwards. The heat flux sensors before the firebreak were set at x = 200 cm, y = 0 cm, z = 4 cm. While the x-coordinate of the heat flow sensors after the firebreak changed according to the width of the firebreak, the y-coordinates (y = 0 cm) and z-coordinates (z = 4 cm) remained constant.

Moreover, dead pine needles collected in Sichuan Province China were used as the fuel in this work. Similar to the previous studies by Silvani [20] and Morandini [8], the fuel was dried in an oven at 60 °C for at least 24 h until the mass stayed the same before the surface fire experiments. The measured data of moisture content of fuel fluctuated around 10% before each experiment, which is comparable to the values in previous studies [7,15,19]. For the uniformity of the fuel bed, the pine needles were carefully and uniformly laid in the three zones before the firebreak and one section after the firebreak into which the fuel bed was divided, where the fuel depth was measured at five random locations in the same zone so that it reached 4 cm. For linear ignition of the surface fire, 5.0 mL ethyl alcohol was evenly sprayed on the edge of the fuel bed. In summary, surface fire experiments in this work were carried out taking 7 wind velocities (0 m/s, 0.5 m/s, 1.0 m/s, 1.5 m/s, 2.0 m/s, 2.5 m/s, 3.0 m/s) and 6 widths of firebreak (10 cm, 15 cm, 20 cm, 25 cm, 30 cm, 35 cm) into account. In this work, two or three repetitive tests were carried out for each set of conditions.

3. Results and Discussions

3.1. Experimental Behavior of Surface Fire Spread

Figure 2 shows the sequences of typical structures for spreading flames over a fuel bed with different wind velocities before the firebreak. For all conditions, the fire could spread steadily to the front of firebreak, and the fire spread behavior was basically similar for fixed wind velocity before the firebreak. As the wind velocity increased, the flame tilted from the burned to unburned fuel surface, even attaching to the fuel surface, and the flame length and flame volume obviously increased. Based on the previous work [29,30], the flame length is the distance from the center of the flame base to the flame tip and the flame angle is defined as the angle between the flame and the unburned surface. The flame length and flame angle during the surface fire spread were obtained by the side-view camera. The average values for a short period of time before the flame front reached the firebreak were used as the characteristic values of flame length and flame angle, as shown in Figure 3. The variations of flame length and angle with time for a short period of time before the flame front reached the firebreak under wind conditions of 0 m/s, 1.5 m/s, and 3.0 m/s, marked with black, red and blue circles were also shown in Figure 3. It can be seen that the flame angle and flame length do not vary much and fluctuate around a specific value over a period of time when the flame front reaches the firebreak. In addition, flame length increased with increasing wind velocity, while flame angle showed the opposite trend. As the wind velocity increased, the flame shifted from tilting towards the burned fuel to adhering to the unburned fuel ahead.

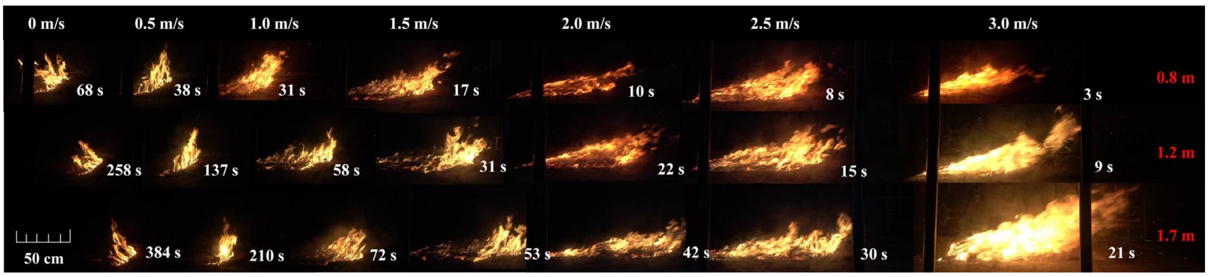

Figure 2. Flame at different wind velocities when the fire front reaches 0.8 m, 1.2 m and 1.7 m from the beginning of the fuel bed.

Figure 4 shows the variation of flame front with time as determined by the characteristic temperature of the thermocouples. The method of determining the position of the flame front of a surface fire by means of the characteristic temperature has also been used by previous work [15,30,31]. It was found that the greater the wind velocity, the faster the flame front moved forward. Moreover, the flame front position showed an essentially linear variation with time, indicating a quasi-steady state during surface fire spread [15,17]. The rate of spread (ROS) of surface fire was obtained from the derivative of the flame front with time as shown in Figure 5. The positions of the flame front at different moments during flame spread at wind velocity of 1.5 m/s, marked with circle were also plotted in Figure 5. From Figure 5, the ROS grows with increasing wind velocity and achieves the maximum value at wind velocity of 3 m/s.

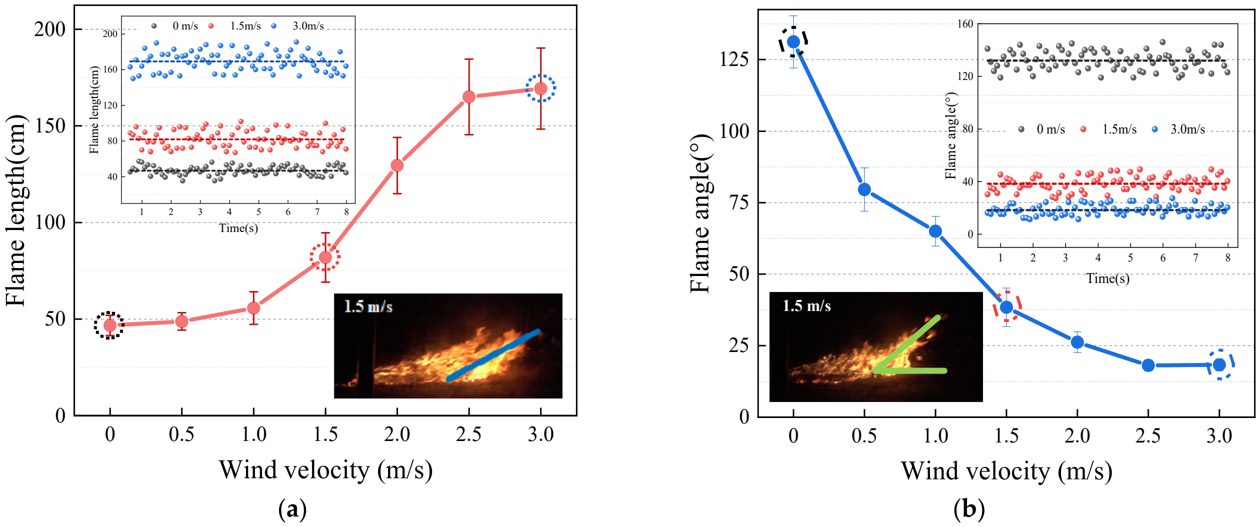

Figure 3. Variation of flame geometry with wind velocity: (**a**) flame length; (**b**) flame angle.

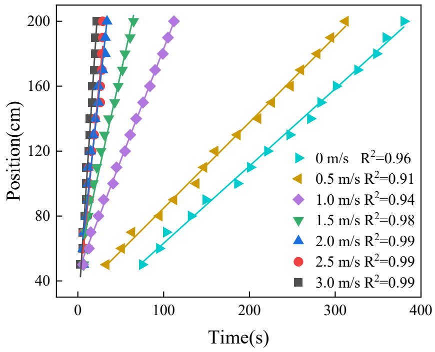

Figure 4. Variation of flame front over time.

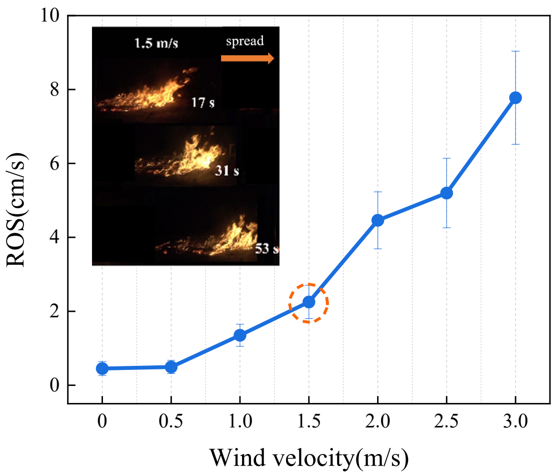

Figure 5. Rate of spread for various wind velocities.

3.2. Effectiveness of Firebreak

For different wind velocities and firebreak widths, different fire spread phenomena were observed after the firebreak, as shown in Figure 6. The surface fire behaviors across the firebreak can be classified into three categories, that is, no ignition, ignition by flame contact and ignition by spot fires. When the wind velocity was low, the flame volume was relatively small, and consequently the firebreaks could successfully prevent the fuel surface after the firebreak from receiving sufficient heat to be ignited. As the wind velocity rose, the flame was elongated and tilted toward the fuel surface, and correspondingly the heat received by the unburned fuel after the firebreak enhanced, possibly resulting in the ignition of fuel after the firebreak by flame contact (marked with red box in Figure 6). When the wind velocity was large enough, the burning fuel could be blown away along the fuel bed, similar to the behavior of spot fires, which ignite the fuel after the firebreak (marked with red circle in Figure 6).

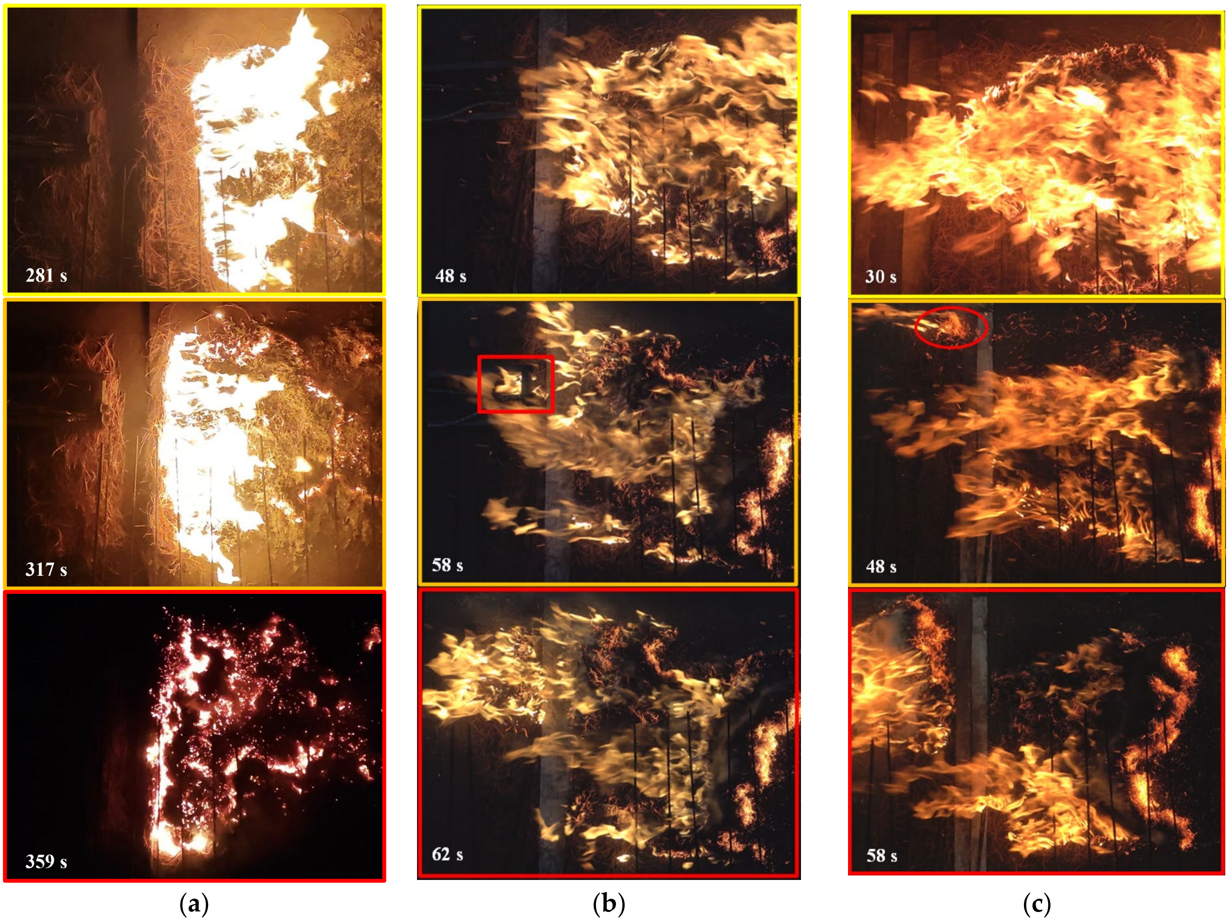

Figure 6. Sequences of typical structures for surface fires spreading across the firebreak: (**a**) no ignition; (**b**) ignition by contact flame; (**c**) ignition by spot fire.

The ignition statistics of a surface fire across the firebreak are summarized in Figure 7. When the wind velocity was not more than 1.0 m/s, the fuel after the firebreak could not be ignited for conditions with different firebreaks. As wind velocity changed from 1.5 m/s to 2.5 m/s, the surface fire could not successfully cross the firebreak for relatively larger firebreak conditions, but the fuel after the firebreak could be ignited by flame contact for relatively narrow firebreak conditions. When the wind velocity increased to 3.0 m/s, the burning fuel could be blown away along the fuel bed, and the fuel behind the firebreak was ignited by spot fire. In summary, the greater the wind velocity and the narrower the firebreak, the more likely the fuel behind the firebreak was to ignite successfully.

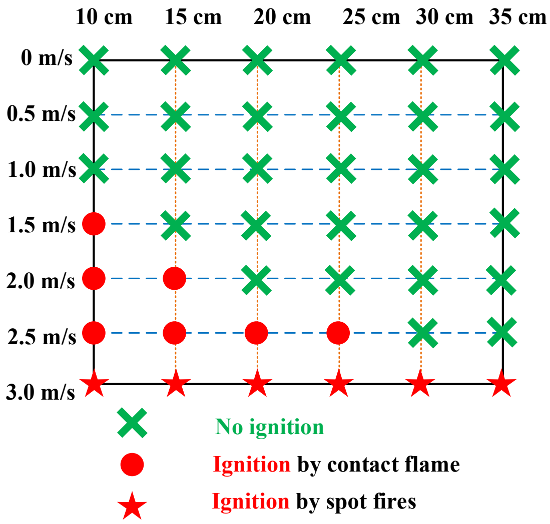

Figure 7. Ignition statistics for a surface fire spreading across the firebreak.

As analyzed previously, the surface fire experiments were investigated by introducing various wind velocities and firebreak widths, and identifying the different situations of not ignited, ignition by flame contact and ignition by spot fire crossing the firebreak. Subsequently, the effectiveness of the firebreak against surface fires was analyzed and compared in detail. According to previous work by Wilson [25], the optimal firebreak is basically related to the fireline intensity I. Additionally, for the ignition conditions by direct contact flame, a simplified model to estimate a fire crossing a firebreak by the fireline intensity I (MW/m) was proposed by Frangieh et al. [22], which can be expressed as follows:

$$L_{fb} \propto 0.36I \tag{1}$$

$$I = HwR \tag{2}$$

where L_{fb} is the firebreak width (m), R is the fire spread rate before the firebreak, H is the flame height, and w is the fuel load consumed by the fire. Figure 8 shows the firebreak width as a function of fireline intensity I, which is compared with predicted results by Equation (1). It can be noted that the slope of the linear fit is larger in this paper compared with the results reported by Wilson [25], which may be due to the differences in the experimental conditions, scale, and fuel between this experiment and Wilsons' work.

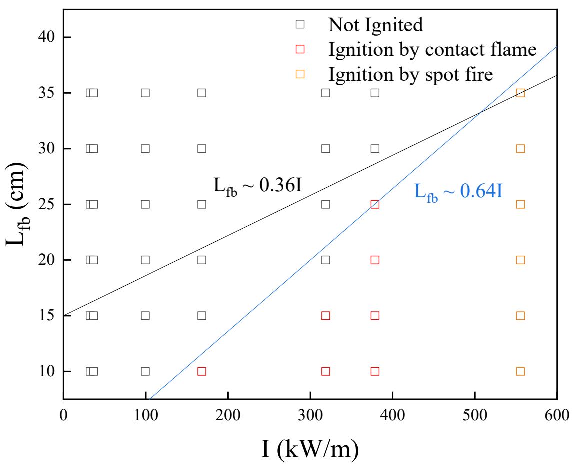

Figure 8. Firebreak width as a function of fireline intensity I.

3.3. Temperature of the Fuel

The temperature development of the fuel before and after the firebreak as a function of time for different ignited conditions with various wind velocities is shown in Figure 9, respectively. For all the conditions, the fuel surface temperature before the firebreak increased rapidly to above the pyrolysis temperature, and then decreased gradually to ambient temperature as the fuel burned out. For not ignited conditions, a significant difference in fuel temperature before and after the firebreak was observed. The fuel temperature after the firebreak varied slightly and was much lower than the pyrolysis temperature of the fuel. However, for the ignited conditions, the fuel temperature increased to exceed the pyrolysis temperature of the fuel, and the fuel was ignited and the flame could continue to spread, which was obviously different from the unignited conditions.

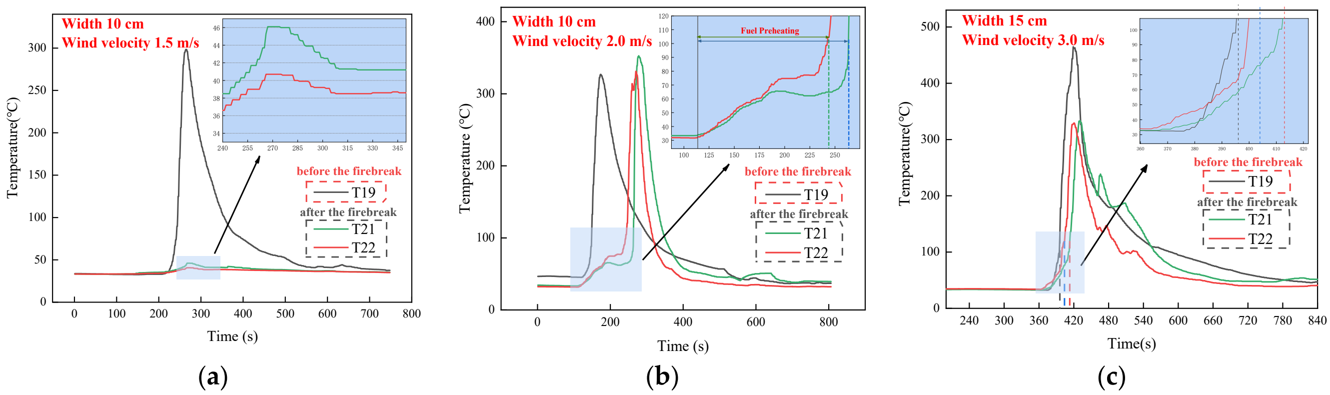

Figure 9. Temperature development of the fuel before and after the firebreak as a function of time for different conditions: (**a**) not ignited; (**b**) ignition by contact flame; (**c**) ignition by spot fire.

Moreover, the variations of the fuel temperature after the firebreak were also different for different ignition conditions, as shown in Figure 9b,c. In the cases of fuel ignited by contact flame, a slow rise in temperature of the fuel after the firebreak before a steep rise was observed, which characterizes the heat absorption process of the fuel before ignition. Nevertheless, only a steep rise in temperature of the fuel after the firebreak was found for ignition conditions by spot fire, where the burning fuel was blown across the firebreak and then ignited the fuel after the firebreak directly. Additionally, for ignition conditions by contact flame, the flame reached the position of each thermocouple in turn, including the thermocouple above the fuel after the firebreak. Whereas, due to the appearance of spot fires, the fuel behind the firebreak could be ignited in different positions, and the fuel temperature rise behind the firebreak may not have followed the same order. As shown in Figure 9c, the temperature of the fuel at 10 cm behind the firebreak rose earlier than that of the fuel at 0 cm behind the firebreak.

The fuel surface temperature before and after the firebreak for not ignited conditions with various wind velocities is shown in Figure 10, where the peak value of temperature is selected as the characteristic value. As can be seen from the figure, the fuel surface temperature increases as the wind velocity grows larger, due to the fact that flame length gets longer and the flame tilts toward the unburned fuel. Additionally, it can be noted that before the firebreak, the maximum temperature exceeded the pyrolysis temperature of the fuel, whereas after the firebreak, the maximum temperature dropped dramatically to below the pyrolysis temperature, and even the fuel temperature in some conditions was only about 40 °C. This observation indicates that the firebreak can effectively prevent the heat transfer from the flame to the unburned surface, and limit the temperature rise of the fuel after the firebreak. Moreover, for a fixed wind velocity, the wider the firebreak, the lower the fuel temperature after the firebreak, and it can decrease with an increase in distance. Additionally, as wind velocity increases, the fuel temperature after the firebreak accordingly increases, which is attributed to the enhanced heat flux from the flame front to the unburned fuel caused by the wind effects.

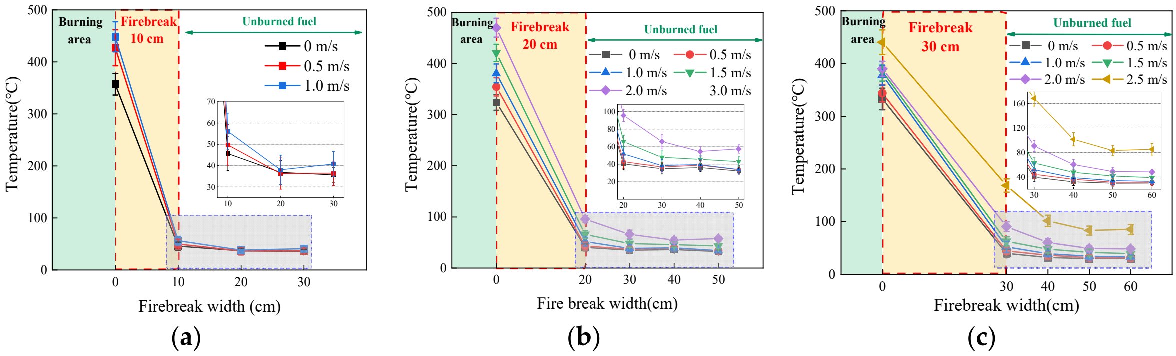

Figure 10. Fuel surface temperature before and after the firebreak for not ignited conditions with various wind velocities and firebreak widths: (**a**) 10 cm width firebreak; (**b**) 20 cm width firebreak; (**c**) 30 cm width firebreak.

The typical temperature variations of the fuel after the firebreak as a function of time for ignited conditions are plotted in Figure 11, in which the dotted line represents the moment the fuel after the firebreak is ignited. As can be seen from Figure 11a, for the ignition conditions by contact flame, the fuel temperature exceeds 253 °C when the fuel after the firebreak is ignited. The greater the wind velocity, the faster the fuel after the firebreak will be ignited. The temperature of the thermocouple closest to the ignition location at the moment of ignition and the maximum temperature of this thermocouple are labeled in the Figure 11b for the ignition conditions by spot fire. From the figure, the thermocouple closest to the ignition location initially does not reach the pyrolysis temperature of the fuel when the fuel after the firebreak is ignited at a certain position, and then gradually increases to the pyrolysis temperature. Also, in the case of ignition by spot fire, the heating of the thermocouples is non-sequential, i.e., the thermocouple closest to the ignition position probably heats up earlier than the thermocouples ahead of it.

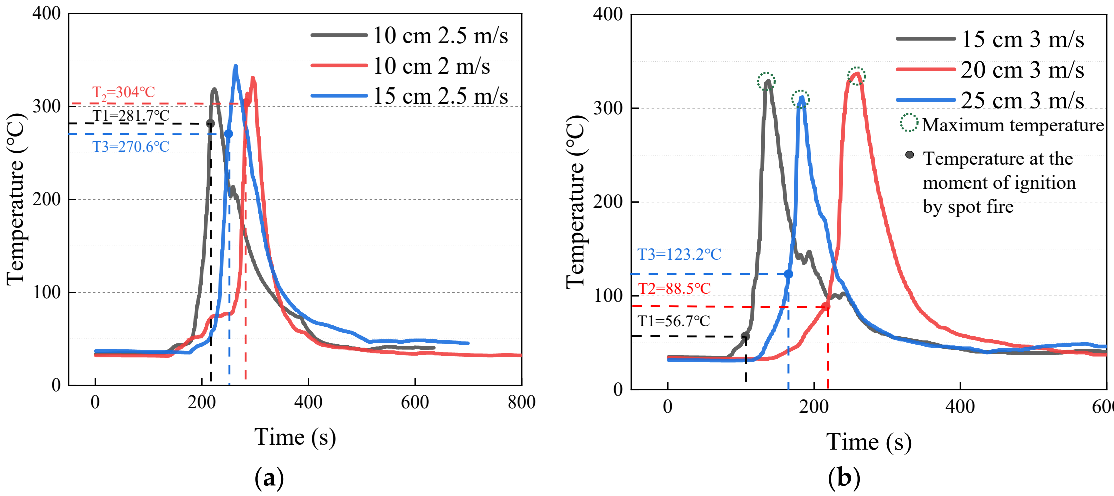

Figure 11. Typical temperature variations of the fuel after the firebreak as function of time for ignition conditions: (**a**) ignition by contact flame; (**b**) ignition by spot fire.

The characteristic temperatures of the fuel after the firebreak for various wind velocity and firebreak conditions are summarized in Figure 12. In this work, the maximum temperature of the first thermocouple behind the firebreak for the unignited cases is concluded in Figure 12, and for the contact ignition cases the temperature at the moment of ignition of the first thermocouple behind the firebreak is compared in Figure 12. Whereas, due to the random character of the spot fire, the temperature of the thermocouple closest to the ignition position at the moment of the ignition and the maximum temperature of this thermocouple are also summarized in Figure 12. Obviously, for the unignited conditions, the fuel temperature after the firebreak was not more than 150 °C and was far less than the pyrolysis temperature of the fuel. As the wind velocity increased, the maximum temperature after the firebreak for unignited conditions increased correspondingly, which indicates that the flame and heat transfer are enhanced by the effects of wind. However, the temperature when the fuel ignited by flame contact and the maximum temperature for ignition conditions by spot fire are all greater than 253 °C. This critical temperature of 253 °C is basically close to the pyrolysis temperature of the fuel.

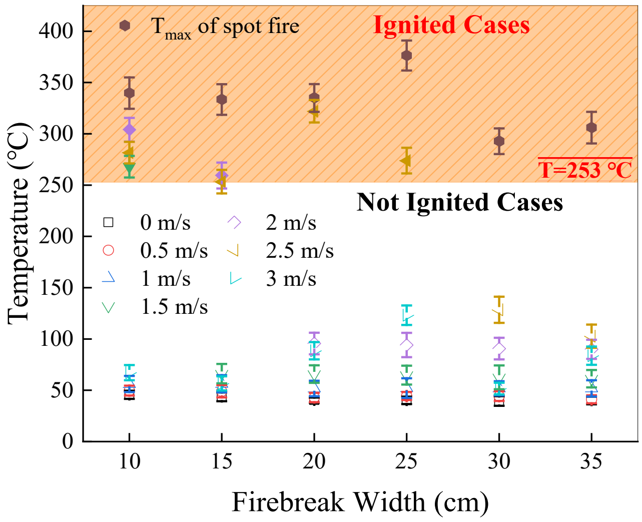

Figure 12. Characteristic temperatures of the fuel after the firebreak for various wind velocity and firebreak conditions.

3.4. Heat Flux

The typical variations of heat flux, including total heat flux (q_{tot}) and radiation heat flux (q_{rad}) over time for different ignition conditions are plotted in Figure 13a, which are obtained by the heat flux sensors. The values of heat fluxes were smoothed by FFT low-pass filtering, and this method was also applied by previous work [14]. It can be seen that as the flame front approaches the heat flux sensor, the value of heat flux before the firebreak increases accordingly until it reaches the maximum value, and then gradually decrease. Moreover, greater total and radiation heat fluxes are observed with increasing wind velocity, which is attributed to the fact that the flame length is elongated and the flame tilts toward the unburned fuel under conditions of increasing wind velocity. It was found that when the flame fails to spread across the firebreak, the total heat flux and its growth rate after the firebreak were obviously less than that before the firebreak, and a similar variation was also observed in the radiation heat flux. But for the ignition conditions by contact flame, the difference between the growth rates of total and radiation heat fluxes before and after the firebreak was not significant. Due to the removal of the heat flux sensors after the firebreak when the fuel after the firebreak was ignited, the values of total heat flow after the firebreak did not increase to be similar to the region before the firebreak. As the wind velocity increased to 3.0 m/s, which was the ignition conditions by spot fire, the total and radiation heat fluxes both exceeded the range of the heat flux meter, which were not described and analyzed in detail in this work.

The heat flux before and after the firebreak for no ignition conditions with various wind velocities and firebreak widths is shown in Figure 13b, in which the heat flux when the fire front reaches the heat flux meter is taken as the characteristic value. It can be observed that whether before or after the firebreak, both corresponding total and radiation heat fluxes increase significantly as the wind velocity rises, which also shows that the heat flux of the unburned fuel can be reinforced by the wind effects. This is attributed to the fact that when the wind is present, the flame length is elongated and the flame tilts toward or even attaches to the fuel surface, which consequently promote the heat transfer. Moreover, when the firebreak appears, the total and radiation heat flux received by the fuel surface after the firebreak significantly decreased, and decreased with the increase of the width of firebreak. Nevertheless, as the width of the firebreak increased, the decrease rate of heat flux received by the fuel surface after the firebreak became smaller.

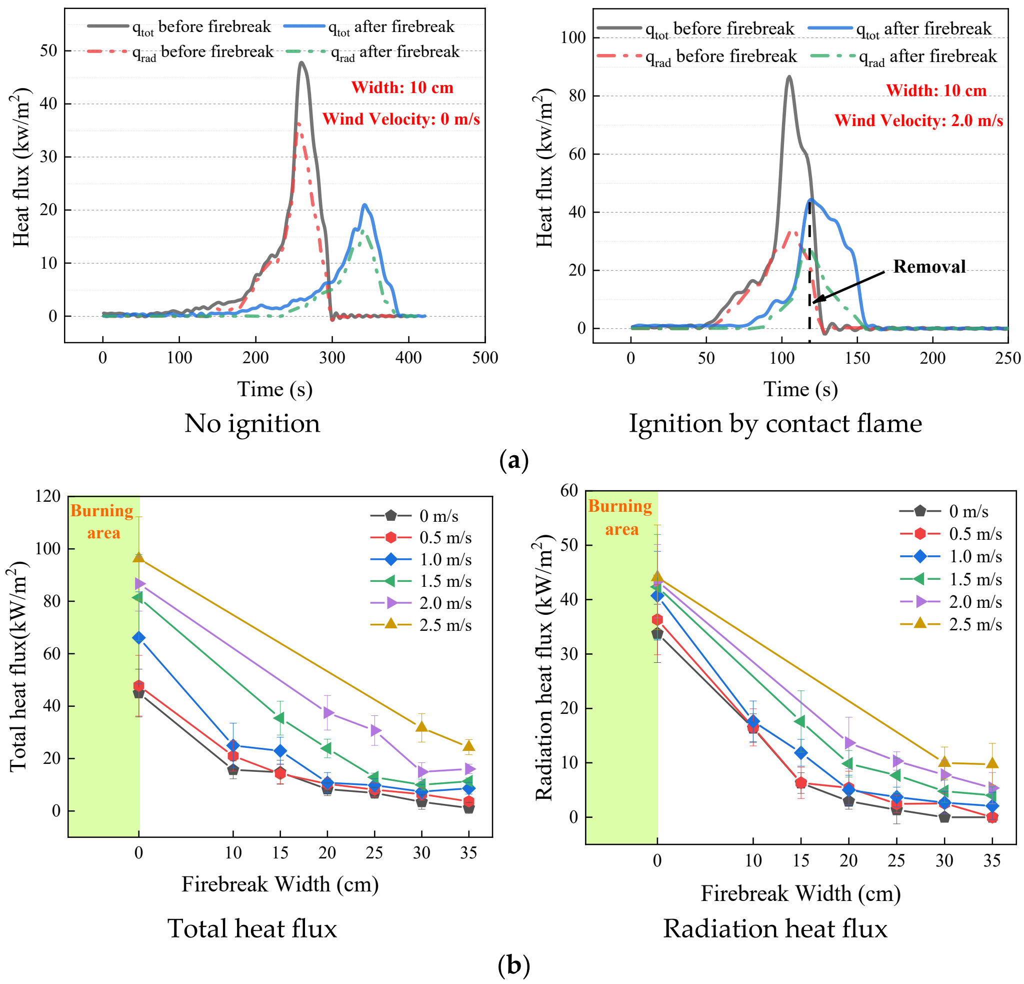

Figure 13. Heat flux before and after the firebreak for different ignition conditions, (**a**) heat flux over time for different ignition conditions and (**b**) heat flux before and after the firebreak for no ignition conditions.

In order to further investigate the effects of firebreak on radiation in the surface fire spread, a simplified model of radiation was analyzed and described. According to the previous observations in this work, the flame can be assumed to be a tilted plane with uniform temperature and emissivity. The radiation heat flux received by a micro-element on the centerline of the fuel bed can be estimated by the following formula [15,17]:

$$\dot{q}_r'' \propto F_{dA_1-A_2}\left(T_f^4 - T_0^4\right) \tag{3}$$

where $\dot{q}_r''$ denotes the radiation heat flux received by the unburned surface, T_f and T_0 are the flame temperature and ambient temperature, respectively, and $F_{dA_1-A_2}$ denotes the view factor between the flame front and the micro-element, which can be expressed as follows for a tilted plane flame [8]:

$$F_{dA_1-A_2} = \frac{1}{2\pi}\left\{\begin{array}{c} \tan^{-1}\left(\frac{1}{C}\right) + X(A\cos\theta - C)\tan^{-1}X + \\ \frac{\cos\theta}{Y}\left[\tan^{-1}\left(\frac{A - C\cos\theta}{Y}\right) + \tan^{-1}\left(\frac{C\cos\theta}{Y}\right)\right] \end{array}\right\} \tag{4}$$

$$A = L_f / w$$

$$C = L_{fb} / w$$

$$X = 1 / \left(A^2 + C^2 - 2AC\cos\phi \right)^{1/2}$$

$$Y = \left(1 + C^2 \sin^2\phi \right)^{1/2}$$

where L_{fb} is the distance between the flame base and the element, w is the width of the fuel bed, L_f is the flame length, which is the length from the flame tip to the flame base and ϕ is the flame angle, which can be defined as the angle between the flame sheet and the fuel surface. The flame length and flame angle before the firebreak can be obtained from the video analyzed frame by frame in a relatively steady stage. Figure 14 plots the view factor $F_{dA_1-A_2}$ as a function of firebreak width for various wind velocities. It can be found that as the firebreak width increased, the view factor $F_{dA_1-A_2}$ decreased significantly, but it showed an opposite trend with wind velocity. This variation is similar to the trend of the experimental results.

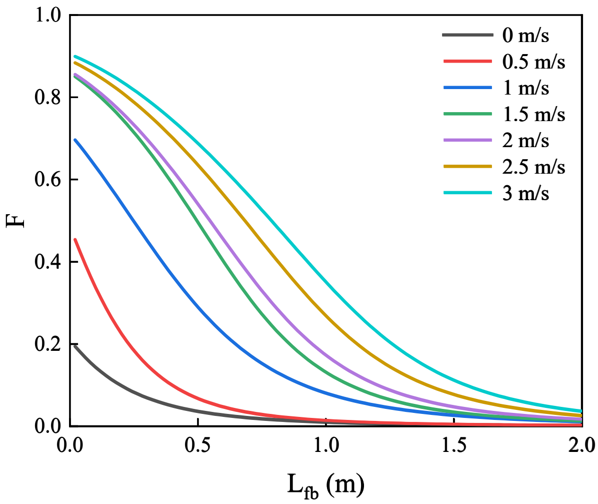

Figure 14. View factor $F_{dA_1-A_2}$ for various firebreak widths and wind velocities.

Many previous works have investigated the variation of heat flux during the spread of surface fires. For instance, Cohen et al. [32] reported that a radiation heat flux of 31 kW/m^2 is the ignition limit of thermally thick wood. However, unlike the ignition of thick wood, the value is lower for vegetation ignition [32]. Additionally, Frangieh et al. [22] numerically studied the effectiveness of a fuelbreak on surface fire spread, and found that in wind driven cases, the heat transfer by convection and radiation both contribute to the ignition process. Mell et al. [33] comparatively analyzed the effects of convection and radiation heat flux on fire spread by computational fluid dynamics (CFD) simulation of a fire spreading through an excelsior fuel bed in the absence of an ambient wind. In this work, heat transfer of radiation heat flux is analyzed and compared. However, the total heat flux received by the fuel surface after the fuel break was greater than the radiation, especially in conditions of greater wind velocities as compared in Figure 13b, which also demonstrates the importance of convection in surface fire spread. Therefore, the characteristic total heat fluxes after the firebreak for various wind velocity and firebreak conditions are presented and compared in this work, as shown in Figure 15, which shows the maximum total heat flux for the unignited condition and the total heat flux when the fuel ignited by flame contact, respectively. It can be noted that for the unignited condition, the maximum total heat flux after the firebreak is not more than 43 kW/m^2, while the total heat flux after the firebreak when the fuel ignited is greater than 43 kW/m^2 for ignition conditions by contact flame. In addition, for unignited conditions, the maximum total heat flux after the firebreak increases with the wind velocity, but shows an opposite trend with firebreak width.

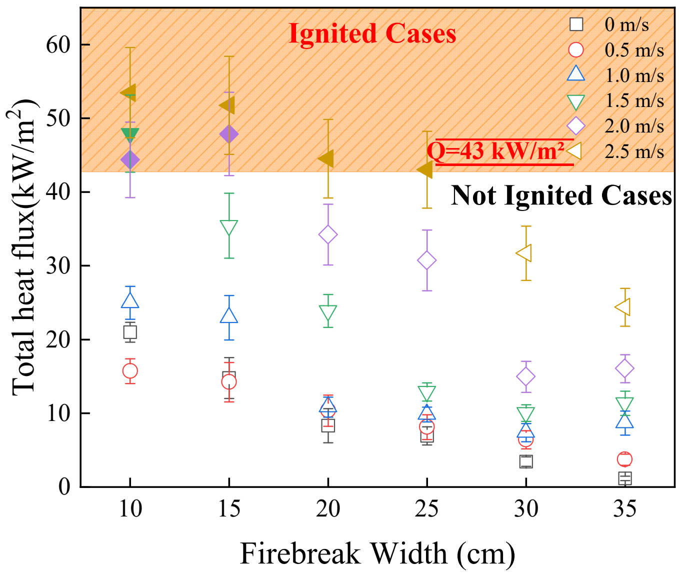

Figure 15. Characteristic total heat flux after the firebreak for various wind velocity and firebreak width conditions.

4. Conclusions

In the present paper, a series of laboratory scale experiments were conducted to explore the behaviors of a surface fire spreading across a firebreak under different wind velocities. The behaviors of a surface fire spreading across a firebreak under different wind velocities are classified into the three following categories: no ignition, ignition by flame contact and ignition by spot fires. A linear relationship between the threshold of firebreak width and the fireline intensity was obtained, and the linear fitting coefficient in this paper is larger than the results reported by Wilson (0.36). The fuel temperature and the heat flux received by the fuel before and after firebreak were quantitatively compared and analyzed for various wind velocity and firebreak width conditions. Moreover, when the fuel temperature (253 °C) and the heat flux received by the fuel considering the radiation and convection (43 kW/m^2) after firebreak exceed a threshold value, the surface fire can successfully cross the firebreak. A further study is in progress to investigate the effectiveness of a firebreak on the surface fire spreading under the combined effects of wind and terrain slope.

In this paper, only the wind velocity effects on surface fire across the firebreak were taken into account, while the effects of fuel and slope were not considered, which may lead to certain limitations of the study results. Therefore, a further study is in progress to investigate the effects of fuel type and topography, and the co-effects of slope and wind on surface fire spread across the firebreak.

Author Contributions: Conceptualization, H.G.; formal analysis, H.G., Z.Y. (Zhengyuan Yang), Z.Y. (Ziqun Ye) and D.X.; investigation, H.G.; methodology, Y.G.; writing—original draft, H.G.; Writing—review & editing, Y.G. and Y.Z. All authors have read and agreed to the published version of the manuscript.

Funding: This research was funded by the National Key R&D Program of China (No. 2022YFC3005704), the National Natural Science Foundation of China (NSFC) (No. 52108478), and the Sichuan Science and Technology Program (No. 2022YFS0533).

Data Availability Statement: The data presented in this study are available on request from the corresponding author.

Acknowledgments: The authors would like to thank the National Key R&D Program of China, the National Natural Science Foundation of China (NSFC) and the Sichuan Science and Technology Program for supporting this work.

Conflicts of Interest: The authors declare no conflict of interest.

References

1. Thomas, G.; Rosalie, V.; Olivier, C.; Antonio, L.P. Modelling forest fire and firebreak scenarios in a mediterranean mountainous catchment: Impacts on sediment loads. *J. Environ. Manag.* **2021**, *289*, 112497. [CrossRef]
2. Viegas, D.X.; Simeoni, A.; Xanthopoulos, G.; Rossa, C.; Ribeiro, L.M.; Pita, L.P.; Stipanicev, D.; Zinoviev, A.; Weber, R.; Dold, J.; et al. *Recent Forest Fire Related Accidents in Europe*; Office for Official Publications of the European Communities: Luxembourg, 2009.
3. Molina-Terrén, D.M.; Xanthopoulos, G.; Diakakis, M.; Ribeiro, L.; Caballero, D.; Delogu, G.M.; Viegas, D.X.; Silva, C.A.; Cardil, A. Analysis of forest fire fatalities in southern Europe: Spain, Portugal, Greece and Sardinia (Italy). *Int. J. Wildland Fire* **2019**, *28*, 85–98. [CrossRef]
4. Lin, S.; Liu, Y.; Huang, X. How to build a firebreak to stop smouldering peat fire: Insights from a laboratory-scale study. *Int. J. Wildland Fire* **2021**, *30*, 454–461. [CrossRef]
5. Rothermel, R.C. *A Mathematical Model for Predicting Fire Spread in Wild Land Fuels*; Intermountain Forest & Range Experiment Station, Forest Service, US Department of Agriculture: Ogden, UT, USA, 1972.
6. Viegas, D.X. Slope and wind effects on fire propagation. *Int. J. Wildland Fire* **2004**, *13*, 143–156. [CrossRef]
7. Morandini, F.; Santoni, P.A.; Balbi, J.H. The contribution of radiant heat transfer to laboratory-scale fire spread under the influences of wind and slope. *Fire Saf. J.* **2001**, *36*, 519–543. [CrossRef]
8. Morandini, F.; Simeoni, A.; Santoni, P.A.; Balbi, J.H. A Model for the Spread of Fire across a Fuel Bed Incorporating the Effects of Wind and Slope. *Combust. Sci. Technol.* **2005**, *177*, 1381–1418. [CrossRef]
9. Tachajapong, W.; Lozano, J.; Mahalingam, S.; Weise, D.R. Experimental modelling of crown fire initiation in open and closed shrubland systems. *Int. J. Wildland Fire* **2014**, *23*, 451. [CrossRef]
10. Li, J.; Mahalingam, S.; Weise, D.R. Experimental investigation of fire propagation in single live shrubs. *Int. J. Wildland Fire* **2017**, *26*, 58. [CrossRef]
11. Tachajapong, W.; Lozano, J.; Mahalingam, S.; Zhou, X.; Weise, D.R. Experimental and Numerical Modeling of Shrub Crown Fire Initiation. *Combust. Sci. Technol.* **2009**, *181*, 618–640. [CrossRef]
12. Morandini, F.; Silvani, X. Experimental investigation of the physical mechanisms governing the spread of wildfires. *Int. J. Wildland Fire* **2010**, *19*, 570–582. [CrossRef]
13. Dupuy, J.-L.; Maréchal, A.J. Slope effect on laboratory fire spread Contribution of radiation and convection to fuel bed preheating. *Int. J. Wildland Fire* **2011**, *20*, 289–307. [CrossRef]
14. Silvani, X.; Morandini, F.; Dupuy, J.-L. Effects of slope on fire spread observed through video images and multiple-point thermal measurements. *Exp. Therm. Fluid Sci.* **2012**, *41*, 99–111. [CrossRef]
15. Liu, N.; Chen, H.; Xie, X.; Zhang, L.; Yao, B.; Zhu, J.; Shan, Y. Effect of slope on spread of a linear flame front over a pine needle fuel bed: Experiments and modelling. *Int. J. Wildland Fire* **2014**, *23*, 1087–1096. [CrossRef]
16. Morandini, F.; Silvani, X.; Honoré, D.; Boutin, G.; Susset, A.; Vernet, R. Slope effects on the fluid dynamics of a fire spreading across a fuel bed: PIV measurements and OH* chemiluminescence imaging. *Exp. Fluids* **2014**, *55*, 1–12. [CrossRef]
17. Liu, N.; Wu, J.; Chen, H.; Zhang, L.; Deng, Z.; Satoh, K.; Viegas, D.X.; Raposo, J.R. Upslope spread of a linear flame front over a pine needle fuel bed: The role of convection cooling. *Proc. Combust. Inst.* **2015**, *35*, 2691–2698. [CrossRef]
18. Xie, X.; Liu, N.; Lei, J.; Shan, Y.; Zhang, L.; Chen, H.; Yuan, X.; Li, H. Upslope fire spread over a pine needle fuel bed in a trench associated with eruptive fire. *Proc. Combust. Inst.* **2017**, *36*, 3037–3044. [CrossRef]
19. Morandini, F.; Silvani, X.; Dupuy, J.L.; Susset, A. Fire spread across a sloping fuel bed: Flame dynamics and heat transfers. *Combust. Flame* **2018**, *190*, 158–170. [CrossRef]
20. Silvani, X.; Morandini, F.; Dupuy, J.L.; Susset, A.; Vernet, R.; Lambert, O. Measuring velocity field and heat transfer during natural fire spread over large inclinable bench. *Exp. Therm. Fluid Sci.* **2018**, *92*, 184–201. [CrossRef]
21. Xie, X.; Liu, N.; Raposo, J.R.; Viegas, D.X.; Yuan, X.; Tu, R. An experimental and analytical investigation of canyon fire spread. *Combust. Flame* **2020**, *212*, 367–376. [CrossRef]
22. Frangieh, N.; Accary, G.; Rossi, J.L.; Morvan, D.; Meradji, S.; Marcelli, T.; Chatelon, F.J. Fuelbreak effectiveness against wind-driven and plume-dominated fires: A 3D numerical study. *Fire Saf. J.* **2021**, *124*, 103383. [CrossRef]
23. Zong, X.; Tian, X.; Wang, X. An optimal firebreak design for the boreal forest of China. *Sci. Total Environ.* **2021**, *781*, 146822. [CrossRef]
24. Emmons, H.W. Fire in the forest. In *Fire Research Abstracts and Reviews*; Committee on Fire Research of the Division of Engineering, National Research Council: Washington, DC, USA, 1964.
25. Wilson, A.A. Width of firebreak that is necessary to stop grass fires: Some field experiments. *Can. J. For. Res.* **1988**, *18*, 682–687. [CrossRef]
26. Morvan, D. Numerical study of the behaviour of a surface fire propagating through a firebreak built in a Mediterranean shrub layer. *Fire Saf. J.* **2015**, *71*, 34–48. [CrossRef]

27. Dupuy, J.L.; Morvan, D. Numerical study of a crown fire spreading toward a fuel break using a multiphase physical model. *Int. J. Wildland Fire* **2005**, *14*, 141. [CrossRef]
28. Tachajapong, W.; Lozano, J.; Mahalingam, S.; Zhou, X.; Weise, D.R. An Investigation of Crown Fuel Bulk Density Effects on the Dynamics of Crown Fire Initiation in Shrublands1. *Combust. Sci. Technol.* **2008**, *180*, 593–615. [CrossRef]
29. Rossa, C.G.; Davim, D.A.; Viegas, D.X. Behaviour of slope and wind backing fires. *Int. J. Wildland Fire* **2015**, *24*, 1085–1097. [CrossRef]
30. Guo, H.; Xiang, D.; Kong, L.; Gao, Y.; Zhang, Y. Upslope fire spread and heat transfer mechanism over a pine needle fuel bed with different slopes and winds. *Appl. Therm. Eng.* **2023**, *229*, 120605. [CrossRef]
31. Dupuy, J.L.; Maréchal, J.; Portier, D.; Valette, J.C. The effects of slope and fuel bed width on laboratory fire behaviour. *Int. J. Wildland Fire* **2011**, *20*, 272–288. [CrossRef]
32. Cohen, J.D. Relating flame radiation to home ignition using modeling and experimental crown fires. *Can. J. For. Res.* **2004**, *34*, 1616–1626. [CrossRef]
33. Mell, W.; Simeoni, A.; Morvan, D.; Hiers, J.K.; Skowronski, N.; Hadden, R.M. Clarifying the meaning of mantras in wildland fire behaviour modelling: Reply to Cruz et al. (2017). *Int. J. Wildland Fire* **2018**, *27*, 770–775. [CrossRef]